Field-enhanced chemical short-range order in amorphous $Cu_{50}Ti_{50}$

1995 J. Phys.: Condens. Matter 7 1235

(http://iopscience.iop.org/0953-8984/7/7/005)

J. Phys.: Condens. Matter 7 (1995) 1235–1243. Printed in the UK

Field-enhanced chemical short-range order in amorphous $Cu_{50}Ti_{50}$

Y Onodera

Department of Materials Science, Faculty of Engineering, Tohoku University, Sendai 980–77, Japan

Received 25 July 1994, in final form 31 October 1994

Abstract. Isochronal and isothermal annealing curves of the reversible structural relaxation chemical short-range order, in amorphous $Cu_{50}Ti_{50}$ with and without field (or current) stress are obtained by the resistometric method. The isochronal curves under field are simply compared with those that have undergone the usual furnace annealing. On the other hand, the data of the isothermal curves are analysed in terms of the activation energy spectrum model of two-level systems. The result for two groups of these curves suggests that the reversible structural relaxation is accelerated by power annealing (E = 5–50 V m^{-1} corresponding to J = 179–1751 A cm^{-2}).

1. Introduction

In this paper, the author does not distinguish between the term 'field' and 'current', and has used the former term for convenience because it remains unclear whether electric 'field' and/or 'current' affect the various relaxation phenomena in metallic glasses or not.

Although much investigation has been made into the effect of the electric field on structural relaxation and crystallization in many amorphous alloys, most of the work uses electric field (pulse or continuous) as a rapid heating method [1–4] to improve some physical properties such as magnetic and mechanical properties [5, 6] or to obtain accurate temperature–time transformation diagrams of metallic glasses [7]. Moreover, the possibility to make use of the metallic glass as the diffusion barrier has been examined in the technology of integrated circuit metallization, because a metallic glass is expected to be a very highly resistive material to electromigration owing to its absence of grain boundaries [8]. On the other hand, there are few investigations, except for Joule heat, to examine the effect of the field stress itself on the structural relaxation and crystallization in amorphous alloys. Lai *et al* [9] reported that the microstructures of amorphous $Fe_{75}Si_{10}B_{15}$ alloys were affected somewhat by electropulsing.

Mizubayashi *et al* [10] investigated the effect of the direct electric current on the kinetic behaviour of the irreversible topological short-range order (TSRO), and crystallization in amorphous $Cu_{50}Ti_{50}$. They concluded that these relaxations are drastically enhanced by electric field above a critical value. However, its physical mechanism still remains unknown.

In preliminary studies by the author and co-workers, it has been found that there is a difference in the kinetics of the crystallization in $Fe_{84}B_{16}$ expressed by a Johnson–Mehl plot [11] between the usual furnace annealing and the power annealing under the alternating electric current of 50 Hz (538, 2250 A cm^{-2}), and that the alternating (50 Hz) electric field (E = 6.8–11.6 V m^{-1}) [12] and direct electric field (E = 5–10 V m^{-1}) [13] seem to

0953-8984/95/071235+09$19.50

enhance the chemical short-range order (CSRO) in $Cu_{50}Ti_{50}$. The purpose of the present study is to confirm these preliminary results, especially for the effect of electric field itself on the CSRO (reversible structural relaxation) in amorphous $Cu_{50}Ti_{50}$.

2. Experimental details

The amorphous $Cu_{50}Ti_{50}$ has been prepared in a ribbon form by melt spinning in an argon atmosphere from a mother ingot. The purity of the starting elements is 99.99 wt.% Cu and 99.947 wt.% Ti, respectively. Average thickness of the ribbon is 10–20 μm and the width is 1.2–1.5 mm. No crystallization was detected in x-ray diffraction patterns for any as-prepared ribbon.

The ends of the ribbon were split, with the split ends being used as electrical contacts. The central unsplit section of about 3 cm in length, served as a specimen that was sandwiched between two mica plates of thickness about 0.2 mm. The four split ends were joined with external circuits (copper wires) by screw-loaded contacts as shown in figure 1.

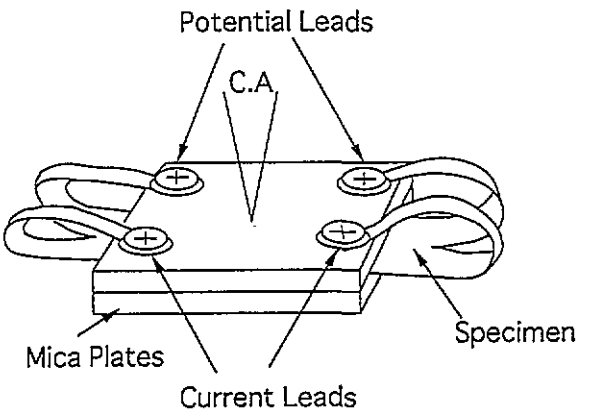

Figure 1. Specimen arrangement to measure the change in electrical resistance after various heat treatments.

The specimen was mounted with the mica plates on a quartz holder and placed in a vacuum-tight quartz tube. After evacuation down to pressures around 3×10^{-3} Pa, it was filled with purified argon gas. Heat treatment such as annealing and quenching was performed with this tube. Two different furnaces were prepared for annealing to attain to an annealing temperature from the reference temperature (273 K) in as short a time as possible. First, the quartz tube was inserted into the furnace set at 773 K, and held for about 60 s or less. Next, it was quickly transferred into the second furnace, the temperature of which was set at a prescribed annealing temperature (lower than 773 K). The duration of an annealing time was 20–30 min for most heat treatments. After quenching from the annealing temperature into iced water, the specimen was left for about 20 min until it had cooled down to 273 K. Then, the resistivity change was measured at this reference temperature by the four-probe DC method under a current density of 20 A cm^{-2}. An isochronal or isothermal annealing curve was obtained by repeating this process for the same specimen set at the beginning of measurement.

The specimen temperature was measured with a thermocouple (chromel–alumel 0.5 mm in diameter) pressed onto a mica plate (figure 1) and extracted from the quartz tube. In this case, the actual specimen temperature becomes necessarily higher than that measured when an additional heat, such as Joule heat, is evolved in the specimen. The direct electric current was supplied using the current lead (figure 1) during power annealing from a constant current source stabilized within ±0.1%.

3. Results

Two types of annealing relaxation were made:

(i) Isochronal annealing. As-prepared specimens were subjected to heat treatment in the temperature region from around 333 to 643 K, in which every thermal relaxation may be involved (crystallization temperature 635 K). The annealing time was 30 min at each annealing temperature.

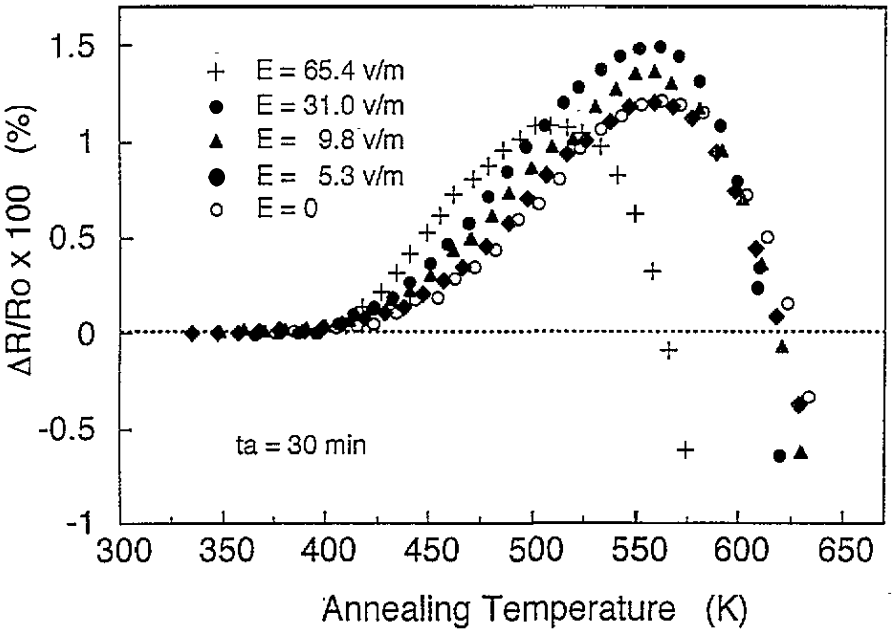

Figure 2. Isochronal annealing curves under various field strengths.

The fractional changes normalized by the value of the resistance of as-prepared specimen $\Delta R\ (= R - R_0)/R_0 \times 100$ was plotted against annealing temperatures as shown in figure 2. All the curves obtained under various field strengths show qualitatively the same behaviour. However, except in the case of the weak field ($E = 5.3$ V m^{-1}), the other curves ($E = 9.8$, 31.0, 65.4 V m^{-1}) do not coincide with that of $E = 0$. The temperature corresponding to the peak values seems to be the same among these four curves ($E = 0$, 5.3, 9.8, 31.0 V m^{-1}). Furthermore, if we compare the two curves ($E = 9.8$, 31.0 V m^{-1}) with the curve of $E = 0$, the value of $\Delta R/R_0 \times 100$ increases with increasing field strength in the temperature range below 580 K. On the other hand, above this temperature, the values of these curves decrease rapidly and become negative. In the case of the strongest field ($E = 65.4$ V m^{-1}), the peak

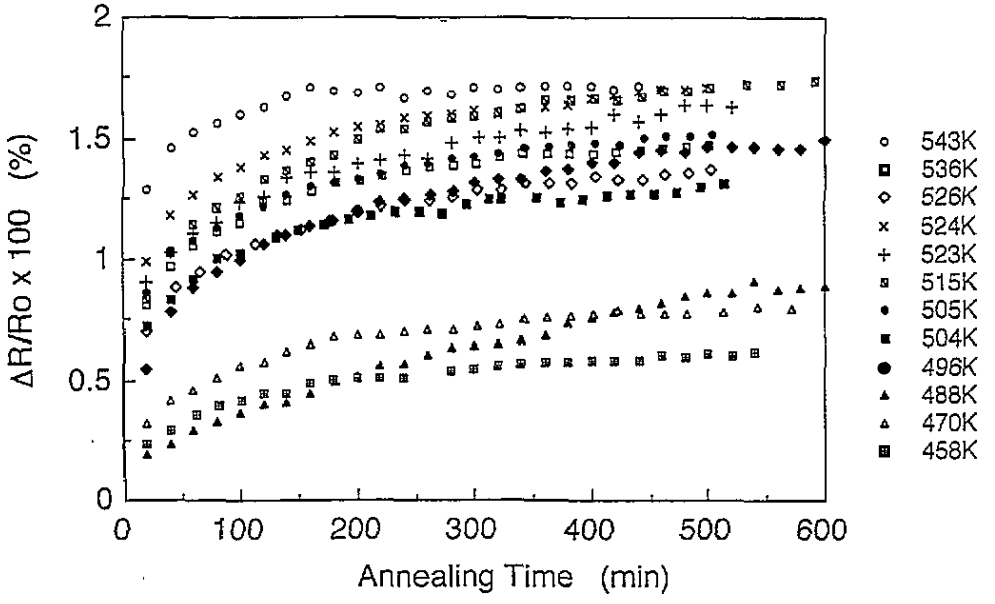

Figure 3. Isothermal annealing curves at various temperatures without field stress.

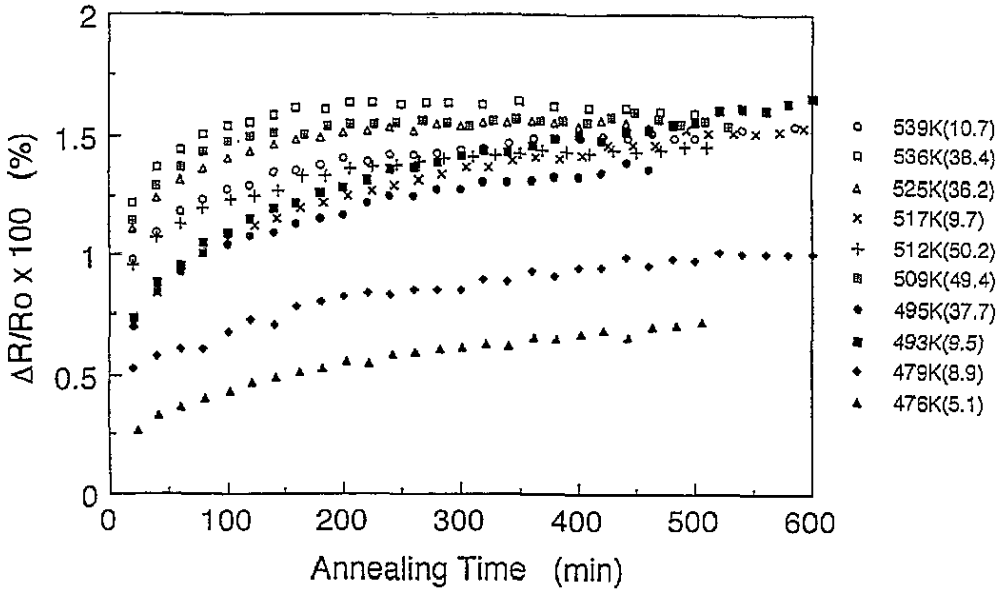

Figure 4. Isothermal annealing curves at various temperatures under various field strengths. The figures in parentheses by the temperatures show the field strength applied during annealing.

value is shifted remarkably to the lower-temperature side and becomes smaller than that of the curve of $E = 0$.

(ii) Isothermal annealing. Figures 3 and 4 show isothermal annealing curves without and with field stress at various temperatures and under various field strengths. In these figures, the fractional change ($\Delta R/R_0 \times 100$) was plotted against the annealing time t. In contrast

to the isochronal curves, no distinct tendencey, which may depend on such parameters as annealing temperature and field strength, can seemingly by recognized in these curves. This may be due to the fact that the isothermal curve is more sensitive to sample homogeneity used in the present experiment than the isochronal curve. Therefore, it cannot be definitely determined from these isothermal curves, by the same method of simply comparing the curves with and without field stress, whether there is some effect of the field stress or not. Another method was then employed here to avoid this disadvantage; it is to use the derivative of these curves, which is insensitive to the absolute value of the fractional change ($\Delta R/R_0 \times 100$), as described below.

4. Discussion

(i) Isochronal curves. In the case of power annealing, the specimen temperature measured is apparent because it is very difficult to estimate the increase in the specimen temperature due to Joule heating without disturbing the thermal distribution in the specimen. In particular, in the present experimental condition, the actual specimen temperature must necessarily become higher than the measured one because of the arrangement of the thermocouple as described in section 2.

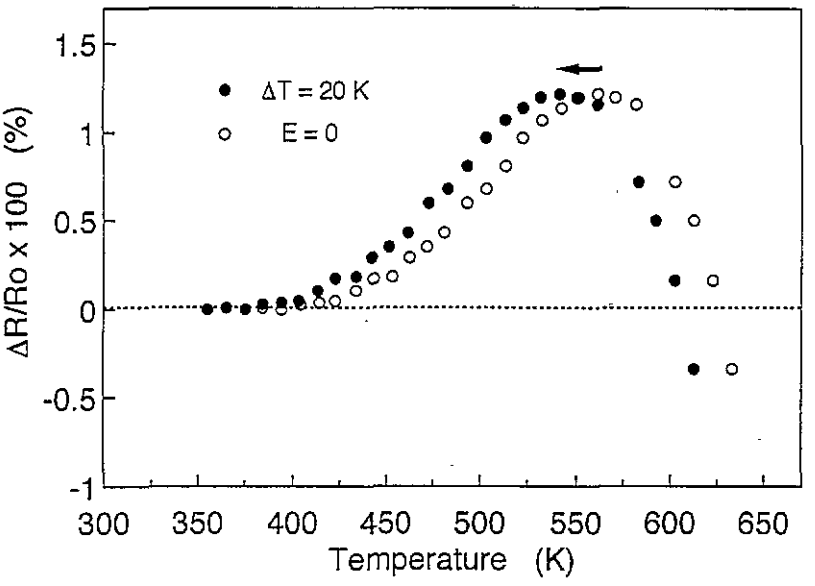

Figure 5. The relation between an isochronal annealing curve without field stress (○) and that assuming with only the additional temperature increase caused by Joule heat (●) which cannot be accurately estimated by the present method for temperature measurement.

If only this additional temperature increase exists and there is no effect of the field itself on CSRO, then, the relation between the isochronal curves with and without field stress is schematically represented in figure 5. The curve with field stress (●) can be simply obtained by shifting the temperature axis of the curve without field stress (○) to a degree of ΔT to the lower-temperature side. However, none of the four curves under field stress shown in

figure 2 fits this case. Then, the behaviour of each curve in figure 4 can be explained as follows: (*a*) $E = 5.3$ V m^{-1}; the field strength is too weak to affect the relaxation and the temperature increase due to Joule heat is not so large, so that it coincides fairly well with the curve of $E = 0$. (*b*) $E = 9.8, 31.0$ V m^{-1}; the peak temperatures of these curves do not shift to the lower-temperature side and the peak values themselves become large compared with the curve of $E = 0$. This result strongly suggests the reversible CSRO is enhanced by field stress since it has been known [14, 15] that the electrical resistivity increases with proceeding of CSRO. (*c*) $E = 65.4$ V m^{-1}; since the field strength probably exceeds the critical value of the field-enhanced TSRO found by Mizubayashi *et al*, the negative values begin to contribute at a lower temperature range than those of other curves. Nevertheless, the values in the low-temperature region become the highest ones if compared with another curve, which means the enhancement of CSRO becomes large with increasing field strength.

(ii) Isothermal curves. Since the kinetic behaviour of CSRO in the present experiment does not systematically depend on the annealing temperature as shown in figure 3 even for the case of $E = 0$, it becomes more difficult to distinguish the effect of electric field itself from that apparently due to Joule heat. Then, we analysed these isothermal data by using a two-level system (TLS) model with activation energy spectrum (AES). Gibbs *et al* [16] often applied such a model to explain various phenomena associated with the structural relaxation in metallic glasses. According to this model [17–19], a TLS (figure 6) with the energy difference Δ separated by the activation energy E is distributed in a specimen with different values of E and Δ as a relaxation centre. Thus, the property change ΔP due to the structural relaxation or crystallization in metallic glass can be described as

$$\Delta P = \int_0^\infty \Theta(E, \Delta, T, t)c(E, \Delta)q(E, \Delta)\,\mathrm{d}E\,\mathrm{d}\Delta \tag{1}$$

where Θ is the characteristic annealing function, $q(E, \Delta)$ is the number density of TLS in the range E and Δ to $E + \mathrm{d}E$ and $\Delta + \mathrm{d}\Delta$, and c is the coupling function defined by the unit change in physical property caused by a relaxation of a TLS with activation energy E and Δ.

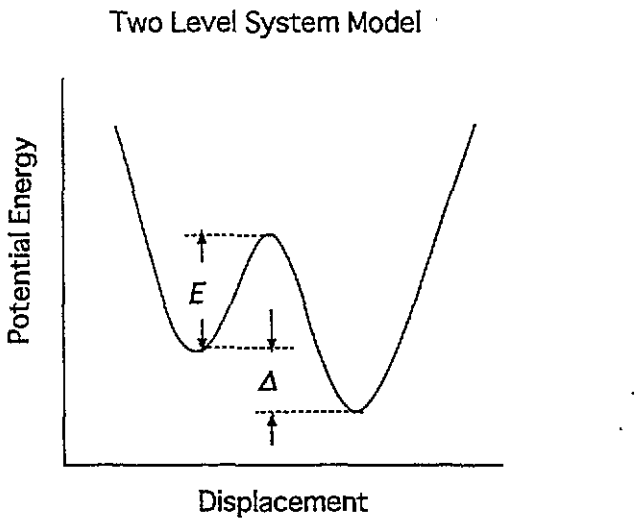

Figure 6. Potential energy of atoms versus configurational variable in a two-level system model.

The characteristic function, which gives the probability that a relaxation process with activation energy E has taken place after time t at temperature T in the TLS of energy splitting Δ, is expressed by

$$\Theta = 1 - \exp\{-\nu t \exp(-E/kT)[1 + \exp(-\Delta/kT)]\} \tag{2}$$

where ν is the attempt frequency and k is the Boltzmann constant.

If we consider only the reversible component of the structural relaxation, we can consider the group of two-level systems that fulfil the condition $\Delta \ll kT_{max}$, where T_{max} is the maximum temperature used in the present experiment. When the function Θ is approximated by the step function, that is, $\Theta = 1$ for E_0 $(= kT \ln t) \geqslant E$ and $\Theta = 0$ for $E_0 \leqslant E$, equation (2) can be rewritten as

$$\Delta P = \int_0^\infty \Theta(E, T, t)c(E)q(E)\,dE \approx \int_0^{E_0} p(E)\,dE \tag{3}$$

where $p(E) = c(E)q(E)$.

If we differentiate (3) by E_0, we obtain

$$d\Delta P/dE_0 = p(E_0) = (t/kT)\,d\Delta P/dt. \tag{4}$$

The right-hand side of (4) can be determined experimentally by measuring the time dependence of the property change ΔP in an isothermal condition. Namely, the values of $p(E_0)$ can be plotted as a function of E_0.

Baricco *et al* [20] used this relation to analyse their experimental results for the structural relaxation in amorphous FeNiCrPB alloys.

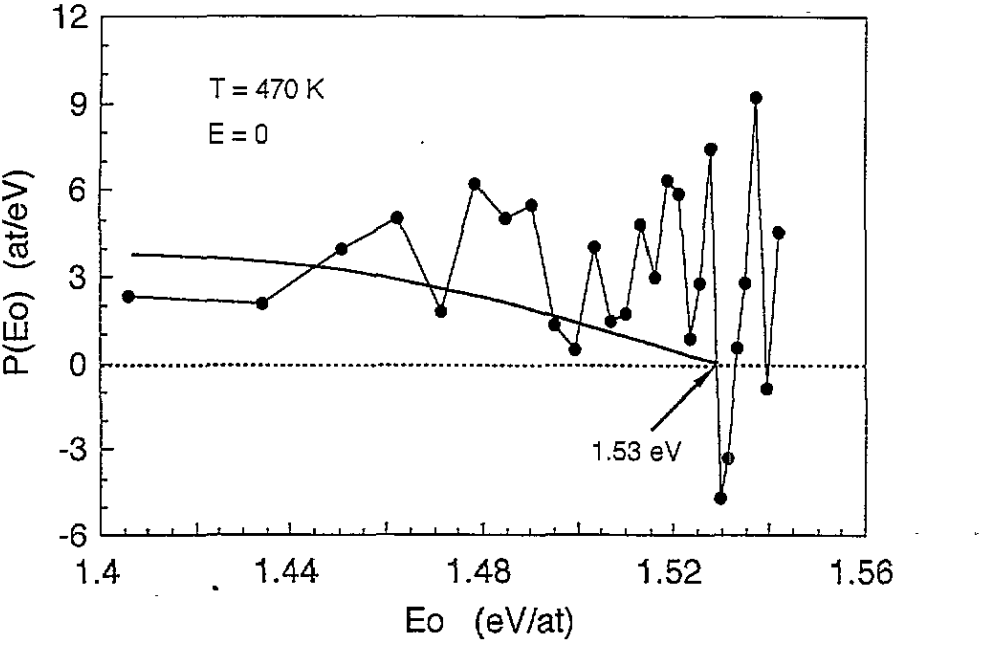

Figure 7. An example of the plot of $P(E_0)$ versus E_0 to obtain the value of E_0 at $P(E_0) = 0$.

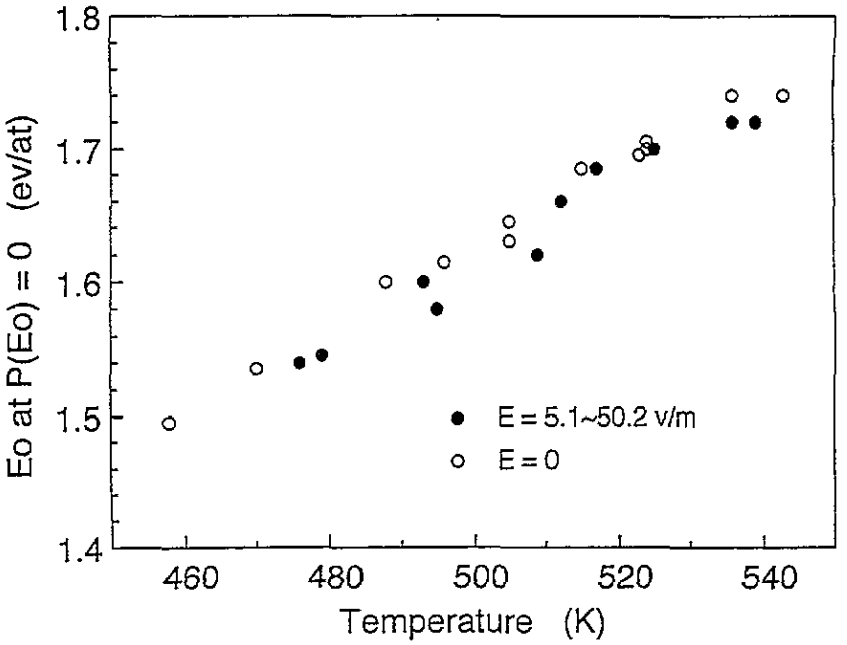

Figure 8. The values of E_0 at $P(E_0) = 0$, obtained from the isothermal curves of figures 3 and 4, versus annealing temperatures to determine the effect of field itself.

A typical plot is shown in figure 7 ($T = 470$ K, $E = 0$). The value of E_0 at $P(E_0) = 0$ may be easily determined from this plot if an isothermal curve behaves completely smoothly during increasing and attaining a constant value. However, the resulting plot from the isothermal curves obtained are rather scattered, especially for the larger E_0. We can understand this situation from (4). The factor t in this equation magnifies the scatter of measured values with increasing annealing time. Therefore, the value of E_0 in the vicinity of the first negative $P(E_0)$ was adopted approximately as the E_0 at $P(E_0) = 0$. In this figure, the solid line is to guide the reader's eye and expresses the ideal one. The resulting values obtained from every curve regardless of whether $E = 0$ or not (figures 3 and 4) are plotted as functions of annealing temperatures as shown in figure 8. If there is no effect of the field on CSRO except the additional temperaure increase due to Joule heat, the values under field stress can be simply obtained by shifting the value of $E = 0$ (○) to the lower-temperature side like along the increasing part for annealing temperature as shown in figure 5. However, the experimental values under field stress (●) are all on the higher-temperature side compared with those of $E = 0$. This suggests again there is some effect of field itself on CSRO, lowering E_0 at $P(E_0) = 0$, and overwhelming that of Joule heat. After all, it is very probable that electric field or current itself enhances CSRO in $Cu_{50}Ti_{50}$ like TSRO [10]. At present, the experimental data may be insufficient to determine whether field stress affects the thermodynamic driving force [21] which facilitates CSRO or such kinetic coefficients as diffusion constant of the atoms related to this relaxation. Hence, it is necessary to investigate how the isothermal curve behaves at larger annealing times in the case of field stress because a quasi-thermodynamic state may ultimately be realized at that time.

5. Conclusion

It has been confirmed that electric field or current certainly enhances the reversible structural relaxation (CSRO) as a result of directly comparing the isochronal curves under various field strengths with the curve without field, and analysing the isothermal curves under various field strengths in terms of two-level system models with an activation energy spectrum.

Acknowledgments

The author wishes to thank Provessor Masumoto, Institute for Materials Research of Tohoku University, for donation of a part of the specimen for the preliminary experiment by Mr Y Nakamura, and is also indebted to Mr E Abe for preparing the sample for this study and carrying out the preliminary measurements.

References

[1] Gibbs M R J, Lee D H and Evetts J E 1984 *IEEE Trans. Magn.* **MAG-20** 1373
[2] Yavari A R, Barrue R, Harmelin M and Perron J C 1987 *J. Magn. Magn. Mater.* **69** 43
[3] Huang D R and Li J C M 1990 *Scr. Metall.* **24** 1137
[4] Kulik T and Matyja H 1991 *Mater. Sci. Eng.* A **133** 232
[5] Allia P, Baricco M, Tiberto P and Vinai F 1993 *Phys. Rev.* B **47** 3118
[6] Allia P, Baricco M, Tiberto P and Vinai F 1993 *Appl. Phys. Lett.* **63** 2759
[7] Zaluski L, Zaluska A, Kopcewicz M and Schulz R 1991 *J. Mater. Res.* **6** 1028
[8] Chisholm M F, Aaron D B, Wiley J D and Perepezko J H 1988 *Appl. Phys. Lett.* **53** 102
[9] Lai Z H, Conrad H, Chao Y S, Wang S Q and Sun J 1989 *Scr. Metall.* **23** 305
[10] Mizubayashi H and Okuda S 1989 *Phys. Rev.* B **40** 8057
[11] Onodera Y and Hirano K 1983 *Amorphous Material-Physics and Technology* ed Y Sakurai (Editorial Committee of the Special Project Research on Amorphous Materials) p 59, unpublished
[12] Nakamura Y 1985 *BS Thesis* Tokohu University, unpublished (in Japanese)
[13] Onodera Y, Abe E and Hirano K 1991 *46th Ann. Meet. Physical Society of Japan* Abstract No 2, p 59, unpublished (in Japanese)
[14] Balanzat E and Hillairet J 1982 *J. Phys. F: Met. Phys.* **12** 2907
[15] Balanzat E, Stanley J T, Mairy C and Hillairet J 1985 *Acta Metall.* **33** 785
[16] Gibbs M R J, Evetts J E and Leake J A 1983 *J. Mater. Sci.* **18** 278
[17] Hygate G and Gibbs M R J 1987 *J. Phys. F: Met. Phys.* **17** 815
[18] Hugate G and Gibbs M R J 1989 *J. Phys.: Condens. Matter* **1** 5021
[19] Hygate G and Gibbs M R J 1990 *J. Phys.: Condens. Matter* **2** 1425
[20] Baricco M, Allia P, Vinai F and Riontino G 1988 *J. Mater. Sci.* **23** 4287
[21] Onodera Y and Hirano K 1986 *J. Mater. Sci. Lett.* **5** 1048